AGU PUBLICATIONS

JGR

Journal of Geophysical Research: Space Physics

RESEARCH ARTICLE

10.1002/2014JA020459

Special Section:
Origins and Properties of Kappa Distributions

Key Points:
- Non-Maxwellian electrons produce both types of kinetic Alfvén solitons
- Exact Sagdeev potential method is used for soliton solution
- Numerical examples are provided to demonstrate the findings

Correspondence to:
P. H. Yoon,
yoonp@umd.edu

Citation:
Masood, W., M. N. S. Qureshi, P. H. Yoon, and H. A. Shah (2015), Nonlinear kinetic Alfvén waves with non-Maxwellian electron population in space plasmas, *J. Geophys. Res. Space Physics*, *120*, doi:10.1002/2014JA020459.

Received 30 JUL 2014
Accepted 5 JAN 2015
Accepted article online 8 JAN 2015

Nonlinear kinetic Alfvén waves with non-Maxwellian electron population in space plasmas

W. Masood[1,2], M. N. S. Qureshi[3], P. H. Yoon[4,5], and H. A. Shah[6]

[1]COMSATS Institute of Information Technology, Islamabad, Pakistan, [2]National Center for Physics, Islamabad, Pakistan, [3]Department of Physics, GC University, Lahore, Pakistan, [4]Institute for Physical Science and Technology, University of Maryland, College Park, Maryland, USA, [5]School of Space Research, Kyung Hee University, Seoul, South Korea, [6]Department of Physics, Forman Christian College, Lahore, Pakistan

Abstract The present work discusses the effects of non-Maxwellian electron distributions on kinetic Alfvén waves in low-beta plasmas. Making use of the two-potential theory and employing the Sagdeev potential approach, the existence of solitary kinetic Alfvén waves having arbitrary amplitude is investigated. It is found that the use of non-Maxwellian population of electrons in the study of kinetic Alfvén waves leads to solutions corresponding to solitary structures that do not exist for Maxwellian electrons. The present investigation solves the riddle of plasma density fluctuations associated with strong electromagnetic perturbations observed by the Freja satellite. The present findings can also be applied to regions of space where various satellite missions have observed the presence of suprathermal populations of plasma species and where the low β assumption is valid.

1. Introduction

The in situ satellite observations of solitary kinetic Alfvén waves (SKAW) have rejuvenated the interest to study the propagation characteristics of these nonlinear coherent structures. For instance, Freja and FAST satellites have shown strong electric spikes with Alfvénic signatures and concomitant ion and electron acceleration in the auroral ionosphere and the magnetosphere [*Carlson et al.*, 1998]. Kinetic Alfvén waves (KAWs) are the extension of magnetohydrodynamic Alfvén waves to the range of short (kinetic) cross-field scales comparable to the ion gyroradius and the electron inertial length. They are also believed to play a significant role in plasma heating, particle acceleration, and anomalous transport, etc. [*Stasiewicz et al.*, 2000]. Kinetic Alfvén waves can interact with the large-scale MHD Alfvén waves and results in the wave energy getting transferred directly from the MHD scales to the kinetic scales [*Voitenko and Goossens*, 2005; *Zhao et al.*, 2011]. Kinetic Alfvén waves can also couple with high-frequency modes such as the ion cyclotron, lower hybrid, and Langmuir waves and be excited by the latter. These waves have also been associated with solar wind turbulence [*Yu et al.*, 1984; *Voitenko et al.*, 2003; *Hall et al.*, 2005].

Solitary kinetic Alfvén waves can be generated by balance between nonlinearity and dispersion when the dispersion relation of ordinary Alfvén waves is modified by the finite Larmor radius effect or the finite electron inertia effect [*Hasegawa and Uberoi*, 1982]. *Kadomtsev* [1965] introduced the idea of using two-potential theory for Alfvén waves in a low-beta plasma. The main premise was that the low-beta assumption allows one to describe the electric field by two potential fields that produce only shear perturbations in the magnetic field. *Hasegawa and Mima* [1976] and *Yu and Shukla* [1978] showed the existence of one-dimensional SKAWs accompanied by only single hump density solitons in a low-beta plasma. The work was later extended to an electron positron-ion plasma, and the formation of solitary waves was shown for different values of beta and positron concentration. *Yinhua et al.* [2000] investigated the SKAWs in a dusty plasma and found that both compressive and rarefactive nonlinear structures could form in such a system. It was also observed that the density humps were cusped and narrower in comparison with the dips.

The satellite missions in astrophysical and space plasmas have frequently observed particle distribution functions that are quasi-Maxwellian up to the mean thermal velocities and possess non-Maxwellian suprathermal tails at high velocities or energies [*Krimigis et al.*, 1983; *Christon et al.*, 1988; *Pierrard and Lemaire*, 1996; *Maksimovic et al.*, 1997]. These so-called nonthermal plasmas are found naturally in the magnetospheres of Earth, Mercury, Saturn, and Uranus, and in the solar wind [*Christon et al.*, 1988;

Maksimovic et al., 1997; *Pierrard et al.*, 2004]. However, the physical origin of these distributions is still under investigation [*Vasyliunas*, 1968; *Scudder and Olbert*, 1979; *Ma and Summers*, 1998; *Pierrard and Lazar*, 2010; *Yoon*, 2012, 2014; *Yoon et al.*, 2012; *Livadiotis and McComas*, 2013].

The observed distributions of charged particles have been well fitted with a generalized Lorentzian distribution, known as the kappa distribution, since it fits both the thermal as well as the suprathermal parts of the observed energy velocity spectra [*Krimigis et al.*, 1983; *Hasegawa et al.*, 1985; *Christon et al.*, 1988; *Pierrard and Lemaire*, 1996; *Maksimovic et al.*, 1997; *Viñas et al.*, 2005; *Baluku et al.*, 2011]. The spectral index κ is a measure of the slope of the energy spectrum of the suprathermal particles forming the tail of the velocity distribution function; the smaller the value, the more suprathermal particles in the distribution function tail and the harder the energy spectrum. Kappa distributions approach the Maxwellian as $\kappa \to \infty$.

The other commonly employed distribution to study the distributions far removed from Maxwellian distribution is Cairns distribution, which was successfully employed to explain the ion-acoustic solitary waves observed by the Freja satellite. *Cairns et al.* [1995] showed that the presence of a non-Maxwellian distribution of electrons could change the nature of ion-acoustic solitary structures to allow for the existence of structures observed by the Freja and Viking satellites [*Bostrom*, 1992; *Dovner et al.*, 1994].

In the present paper, we utilize both the kappa and Cairns models for the electrons to explore the formation of both compressive and rarefactive solitary kinetic Alfvén waves for the first time. If one employs Maxwellian distribution for the electrons, then only compressive soliton solution can be obtained, as indeed indicated by previous works [*Hasegawa and Mima*, 1976; *Yu and Shukla*, 1978].

The present work is organized in the following manner: In section 2, we present the governing set of equations for the problem under consideration and also present the linear dispersion relation for the Kinetic Alfvén wave in the presence of kappa and Cairns distributed electrons. In section 3, we present the nonlinear analysis, whereas in section 4, the results are discussed. Finally, in section 5, we recapitulate the main findings of this paper.

2. Model Equations

We study here the nonlinear propagation of the kinetic Alfvén wave (KAW) for a low (but much higher than the electron to ion mass ratio) but finite beta plasma. We assume that the variation exists in the *x*-*z* plane, where *z* is the direction of the ambient magnetic field. The low-beta assumption allows us to employ the two-potential theory to solve the problem under consideration. In the two-potential theory, we use the two potential fields ϕ and ψ to describe the electric field such that

$$E_x = -\frac{\partial \phi}{\partial x}, \qquad E_z = -\frac{\partial \psi}{\partial z}, \qquad E_y = 0.$$

This implies that only shear perturbations in the magnetic field are present, which are mathematically expressed as $B_z = B_0$ and $B_x = 0$. The quasi neutrality condition for ions and electrons densities leads to $n_e = n_i = n$.

We consider here the non-Maxwellian distribution of electrons. *Cairns et al.* [1995] used a nonthermal velocity distribution function of the form

$$f_\Gamma(v) = \frac{n_0}{3\Gamma + 1} \frac{1}{\sqrt{2\pi v_j^2}} \left(1 + \frac{\Gamma v^4}{v_j^4}\right) \exp\left(-\frac{v^2}{2v_j^2}\right) \tag{1}$$

where Γ is the nonthermal parameter representing the percentage of the nonthermal population of species, n_0 is the equilibrium density, and $v_j = \sqrt{T_j/m_j}$ is the thermal velocity of the species *j*. The distribution function reduces to the Maxwellian distribution form when $\Gamma = 0$. If we take the *Cairns et al.* [1995] distribution (1) for the electrons, replacing the argument v^2 by $v^2 - 2e\psi/m_e$, and integrating over velocity space, one obtains the following expression for the total electron number density:

$$n_e = n_{e0} \left[1 - \Lambda \frac{e\psi}{T_e} + \Lambda \left(\frac{e\psi}{T_e}\right)^2\right] \exp\left(\frac{e\psi}{T_e}\right), \tag{2}$$

where $\Lambda = 4\Gamma/(1 + 3\Gamma)$.

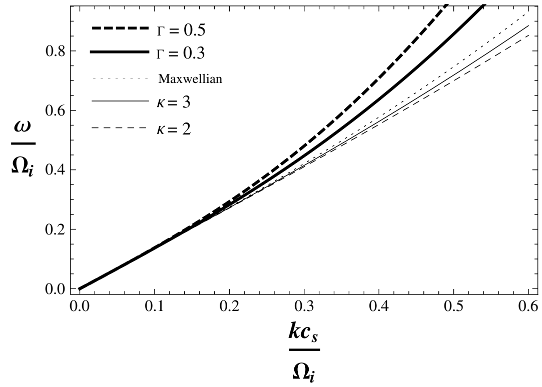

Figure 1. Linear dispersion curves for the kinetic Alfvén wave for Maxellian, *Cairns et al.* [1995], and kappa distributions.

The standard three dimensional isotropic kappa velocity distribution function $f_\kappa(v)$ can be expressed as [*Summers and Thorne*, 1991; *Baluku and Hellberg*, 2008; *Hellberg et al.*, 2009]

$$f_\kappa(v) = \frac{n_0}{\theta^3}\frac{1}{(\pi\kappa)^{3/2}}\frac{\Gamma(\kappa+1)}{\Gamma(\kappa-1/2)}\left(1+\frac{v^2-2e\psi/m_e}{\kappa\theta^2}\right)^{-(\kappa+1)}, \tag{3}$$

where $\theta = \{[(2\kappa-3)T]/\kappa m\}^{1/2}$. In the present paper, we represent temperatures in the unit of energy so that the Boltzmann k_B is set equal to unity. From the definition of kappa distribution function, it is required that $\kappa > 3/2$ [*Pierrard and Lazar*, 2010]. Integrating the kappa distribution over velocity space, one obtains the following expression for the total electron number density:

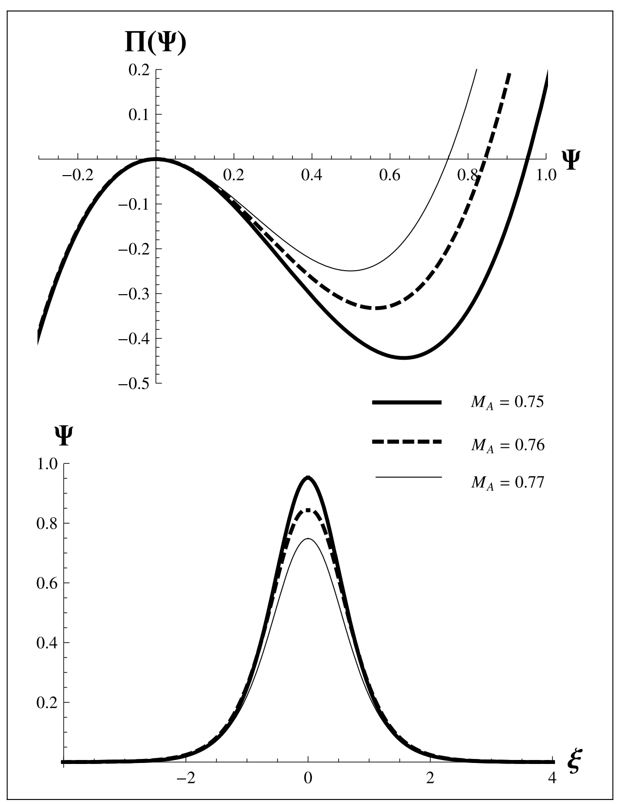

Figure 2. (top) Variation of Sagdeev potential (for kappa-distributed electrons) for different values of Alfvén Mach number $M_A = 0.75$ (solid line), $M_A = 0.76$ (dashed line), and $M_A = 0.77$ (thin line) and (bottom) the corresponding solitary structure are shown. Other parameters are $\kappa = 3$, $\theta = 0.8\ \pi/2$, and $\beta = 0.1$.

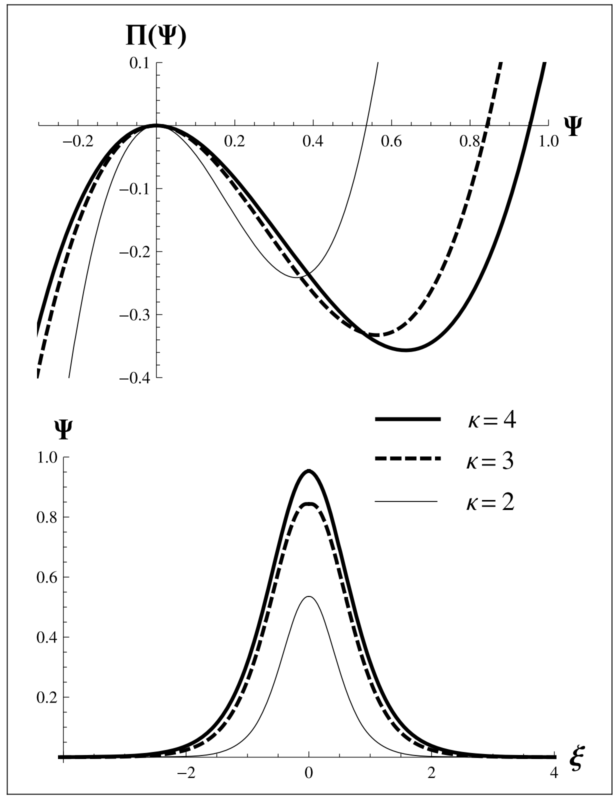

Figure 3. (top) Variation of Sagdeev potential (for kappa-distributed electrons) for different values of $\kappa = 4$ (solid line), $\kappa = 3$ (dashed line), and $\kappa = 2$ (thin line) and (bottom) the corresponding solitary structure are shown. Other parameters are $M_A = 0.76$, $\theta = 0.8\,\pi/2$, and $\beta = 0.1$.

$$n_e = n_{e0}\left[1 - \frac{e\psi}{(\kappa - 3/2)\,T_e}\right]^{-(\kappa-1/2)}, \tag{4}$$

for kappa distribution. It is useful to introduce two parameters, γ and η, where

$$\gamma = \begin{cases} 1-\Lambda & \text{(Cairns)} \\ \dfrac{\kappa-1/2}{\kappa-3/2} & \text{(Kappa)} \end{cases},$$

$$\eta = \begin{cases} 1/2 & \text{(Cairns)} \\ \dfrac{(\kappa-1/2)(\kappa+1/2)}{(\kappa-3/2)^2} & \text{(Kappa)} \end{cases}, \tag{5}$$

The total electron density after the above simplification can be written as

$$n_e = n_{e0}\left(1 + \gamma\Psi + \eta\Psi^2\right), \tag{6}$$

where $\Psi = e\psi/T_e$ is the normalized electrostatic potential. It is worth mentioning here that γ and η in the above equation are defined according to equation (5) for *Cairns et al.* [1995] and kappa distributions, respectively. Following the procedure outlined in the paper by *Hasegawa and Mima* [1976], the component of ion velocity is given by

$$v_{ix} = -\frac{1}{\Omega_i B_0}\frac{\partial^2\phi}{\partial x\partial t}. \tag{7}$$

From Ampere's law [*Hasegawa and Mima*, 1976], we have

$$\mu_0\frac{\partial j_z}{\partial t} = \frac{\partial}{\partial z}\frac{\partial^2}{\partial x^2}(\phi - \psi). \tag{8}$$

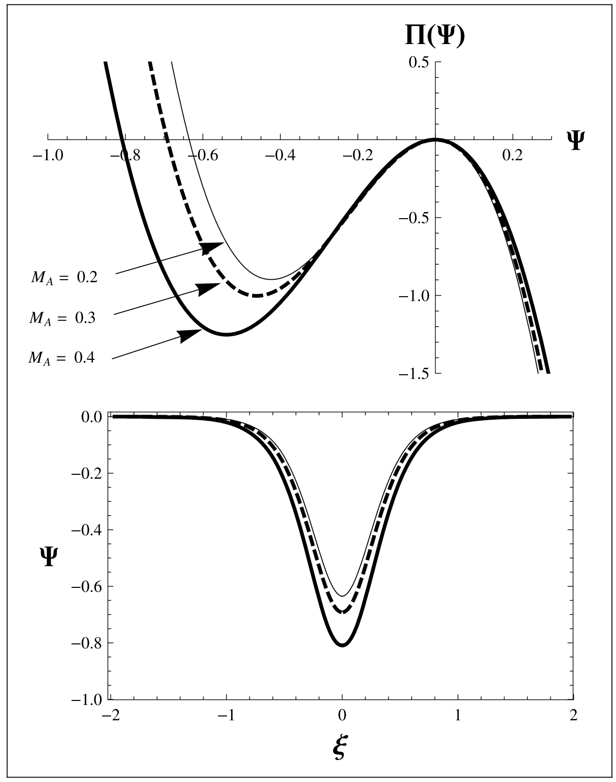

Figure 4. (top) Variation of Sagdeev potential (for kappa-distributed electrons) for different values of Alfvén Mach number $M_A = 0.4$ (solid line), $M_A = 0.3$ (dashed line), and $M_A = 0.2$ (thin line) and (bottom) the corresponding solitary structure are shown. Other parameters are $\kappa = 2$, $\theta = 0.8\,\pi/2$, and $\beta = 0.1$.

The ion continuity equation is given by

$$\frac{\partial n_i}{\partial t} + \frac{\partial}{\partial x}(n_i v_{ix}) = 0 \tag{9}$$

and

$$\frac{\partial j_z}{\partial z} = e\frac{\partial n_e}{\partial t}. \tag{10}$$

The above equation is derived by using the electron continuity equation. Solving equations (7)–(10) yields the following linear dispersion relation:

$$\omega = k_z v_A \sqrt{1 + \frac{\lambda_s}{\gamma}}, \tag{11}$$

where $\lambda_s = k_x^2 \rho_s^2$ is the coupling parameter and $\rho_s = c_s/\Omega_i$ is the Larmor radius defined in terms of the ion-sound speed, $\Omega_i = eB_0/m_i$ is the ion cyclotron frequency, $c_s = \sqrt{T_e/m_i}$ is the ion-sound speed, and $v_A = B_0/\sqrt{\mu_0 n_i m_i}$ is the Alfvén speed. The wave numbers in x and z directions are expressed through the obliqueness angle with respect to the magnetic field and are given by $k_z = k\cos\theta$ and $k_x = k\sin\theta$.

Figure 1 depicts the dispersion relation for the kinetic Alfvén wave for Maxwellian, *Cairns et al.* [1995], and kappa distributions, respectively. Observe that the frequency of the wave under consideration is maximum for *Cairns et al.* [1995], intermediate for Maxwellian, and minimum for kappa distribution. It is observed that decreasing the value of nonthermal population of electrons in the case of *Cairns et al.* [1995] distributed electrons and increasing the value of κ for kappa-distributed electrons shift the frequency toward Maxwellian, which agrees well with the theoretical predictions.

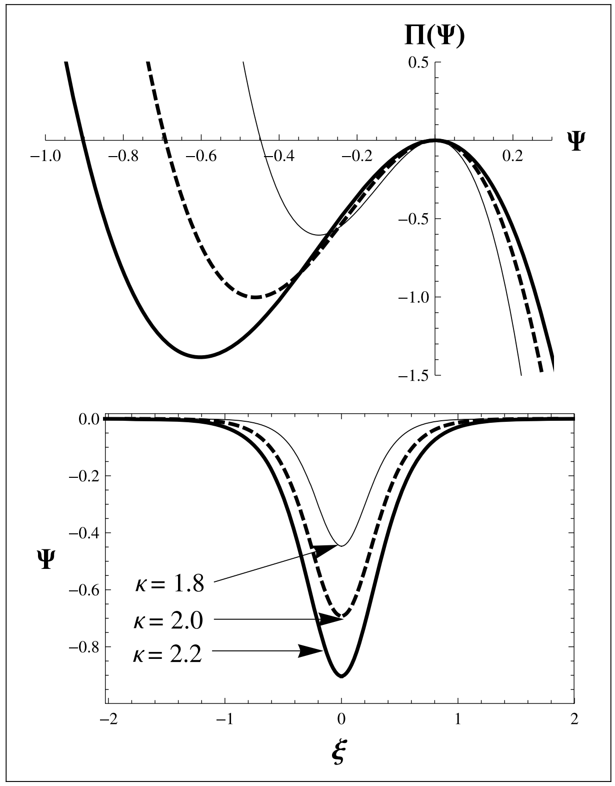

Figure 5. Variation of Sagdeev potential (for kappa-distributed electrons) for different values of $\kappa = 2.2$ (solid line), $\kappa = 2.0$ (dashed line), and $\kappa = 1.8$ (thin line) are shown in the top, whereas the bottom shows the corresponding solitary structure. Other parameters are $M_A = 0.3$, $\theta = 0.8\,\pi/2$, and $\beta = 0.1$.

3. Nonlinear Analysis

In this section, we employ the Sagdeev potential approach to investigate the formation of solitary Kinetic Alfvén waves (SKAW's), and to this end, we shift to a comoving frame of reference in normalized variables

$$\xi = K_x x + K_z z - Mt. \tag{12}$$

The normalized variables are given by

$$n = \frac{n_{e,i}}{n_0}, \quad \Phi = \frac{e\phi}{T_e}, \quad M = \frac{v}{c_s}, \quad \mathbf{K} = \frac{\mathbf{k}c_s}{\Omega_i}, \quad t = \Omega_i t, \tag{13}$$

where n, Φ, M, $\mathbf{K}$, and t are the normalized density, potential, sonic Mach number, wave vector, and the time variable, respectively. Making use of equation (10) in equation (8), we can eventually recast equations (7)–(9) in the following dimensionless form:

$$v_x = K_x M \frac{\partial^2 \Phi}{\partial \xi^2}, \tag{14}$$

$$2K_x^2 K_z^2 \frac{\partial^4(\Phi - \Psi)}{\partial \xi^4} = \beta M^2 \frac{\partial^2 n}{\partial \xi^2}, \tag{15}$$

$$-M\frac{\partial n}{\partial \xi} + K_x \frac{\partial (n v_x)}{\partial \xi} = 0. \tag{16}$$

Integrating equations (14)–(16) and applying the boundary conditions $v_{ix}, \Phi, \Psi \to 0$, and $n_0 \to 1$ as $\xi \to \infty$, we obtain

$$K_x v_x = K_x^2 M \frac{\partial^2 \Phi}{\partial \xi^2}, \tag{17}$$

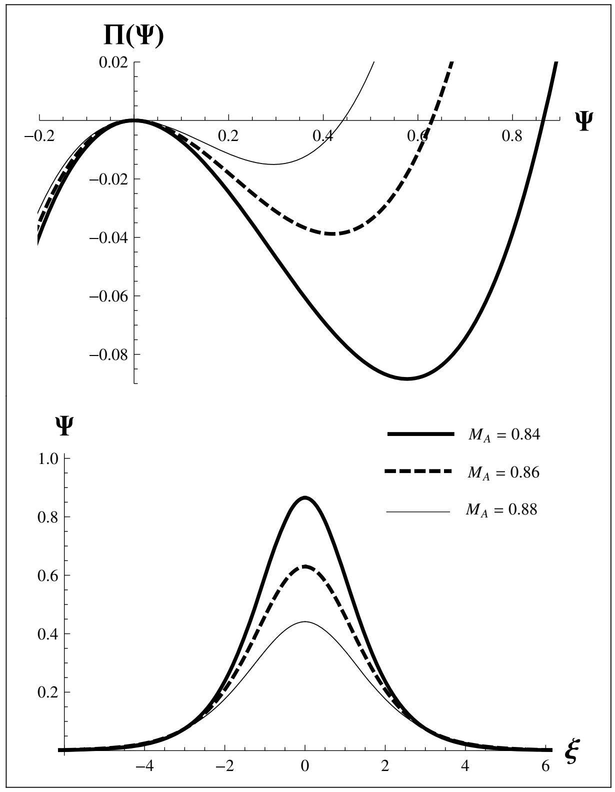

Figure 6. Variation of Sagdeev potential—for *Cairns et al.* [1995] distributed electrons—for different values of Alfvén Mach number $M_A = 0.84$ (solid line), $M_A = 0.86$ (dashed line), and $M_A = 0.88$ (thin line) are shown in the top, whereas the bottom shows the corresponding solitary structure. Other parameters are $\Gamma = 0.1$, $\theta = 0.8\,\pi/2$, and $\beta = 0.1$.

$$2K_x^2K_z^2\frac{\partial^4(\Phi-\Psi)}{\partial\xi^4} = \beta M^2(\gamma\Psi + \eta\Psi^2), \tag{18}$$

$$K_x v_x = M\left(1-\frac{1}{n}\right). \tag{19}$$

Simplifying equations (17) and (19) yields

$$K_x^2\frac{\partial^2\Phi}{\partial\xi^2} = \frac{\gamma\Psi+\eta\Psi^2}{1+\gamma\Psi+\eta\Psi^2}. \tag{20}$$

After simplifying equations (18) and (20), we eventually arrive at an equation that can be expressed in the form of an energy integral through the Sagdeev potential or pseudopotential in the following manner:

$$\frac{1}{2}\left(\frac{\partial\Psi}{\partial\xi}\right)^2 + \Pi(\Psi) = 0, \tag{21}$$

where

$$\Pi(\Psi) = \frac{1}{K_x^2}\left\{-\frac{\gamma}{2}\left(1-\frac{M_A^2}{K_z^2}\right)\Psi^2 + \frac{1}{3}\left[\frac{M_A^2}{K_z^2}\gamma^2 - \eta\left(1-\frac{M_A^2}{K_z^2}\right)\Psi^3\right]\right\}, \tag{22}$$

where $M_A = \sqrt{\beta/2}M$ is the Alfvén Mach number.

4. Results and Discussion

In this section, we numerically investigate the dependence of the Sagdeev potential $\Pi(\Psi)$ versus Ψ for different plasma parameters. In this regard, we have chosen the parameters that are representative of the plasma found in the Saturn's rings, i.e., $n_0 \sim 10^9$ m^{-3}, $T_e = 10$ eV, and $B_0 \sim 0.2\times10^{-4}$T. Our choice of input

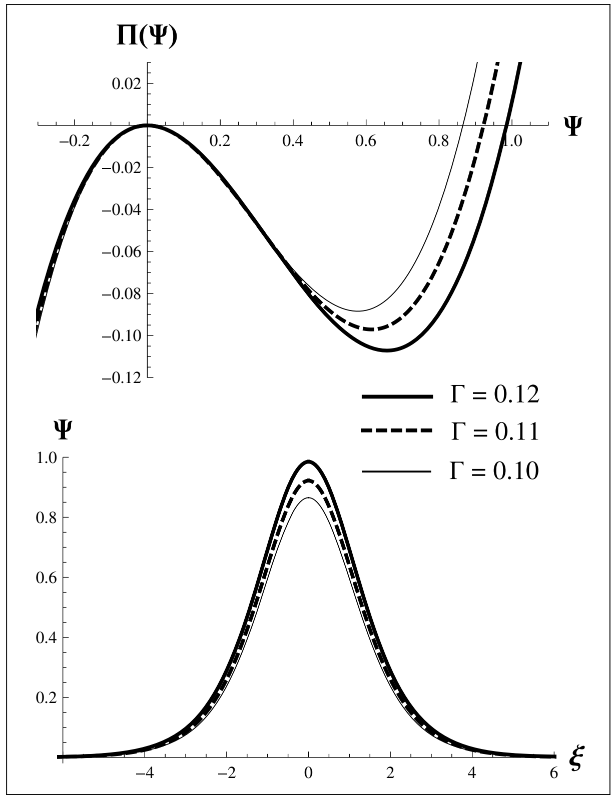

Figure 7. Variation of Sagdeev potential—for *Cairns et al.* [1995] distributed electrons—for different values of $\Gamma = 0.12$ (solid line), $\Gamma = 0.11$ (dashed line), and $\Gamma = 0.1$ (thin line) are shown in the top, whereas the bottom shows the corresponding solitary structure. Other parameters are $M_A = 0.84$, $\theta = 0.8\,\pi/2$, and $\beta = 0.1$.

physical parameters are motivated by satellite missions in the Cronian environment where the presence of nonthermal electrons is reported [*Delamere and Bagenal*, 2008; *Schippers et al.*, 2008]. However, since our formalism is expressed in dimensionless formalism, it is applicable to other space environments. Space plasmas in the near-Earth heliospheric environment are characterized by a range of kappa values, i.e., 2–6. Note also that the nonthermal parameter Γ in the *Cairns et al.* [1995] distribution represents the percentage of the nonthermal electron population, which may have a range of values as well. In short, the basic formalism developed in the present paper is applicable to space plasmas other than the Saturnian ring environment. The value of the plasma beta is considered to be less than 1 in the present discussion, which is true for many regions of space.

4.1. Existence Condition for Compressive Solitary Structures

The condition for positive potential or compressive solitons, which comes from finding the maxima of the Sagdeev potential at $\Psi = 0$, is given by

$$m_1 < M_A < k_z,$$

where

$$\begin{aligned} m_1 &= \frac{1}{2}\frac{k_z^2\left[4\eta + 3\beta + 6\alpha(1+\beta)\right] - \sqrt{k_z^2(4\varpi_1 - 4\beta\varpi_2 + 9\beta^2\varpi_3)}}{\gamma(3+2\gamma)+2\eta}, \\ \varpi_1 &= (3\gamma + 2\eta)^2, \\ \varpi_2 &= \gamma(9 + 6\gamma + 8\gamma^2 - 4\eta) + 6\eta, \\ \varpi_3 &= (1+2\gamma)^2. \end{aligned} \tag{23}$$

Numerical solutions of equation (22) are plotted in Figures 2 and 3 for the compressive solitary structures for kappa-distributed electrons. Figures 2 (top) and 3 (top) explore the variation of the Sagdeev potential

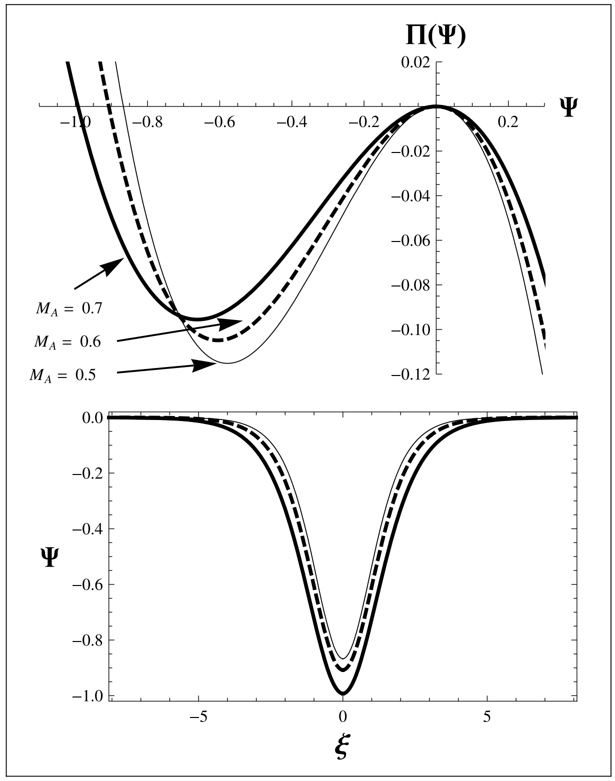

Figure 8. Variation of Sagdeev potential—for *Cairns et al.* [1995] distributed electrons—for different values of Alfvén Mach number $M_A = 0.7$ (solid line), $M_A = 0.6$ (dashed line), and $M_A = 0.5$ (thin line) are shown in the top, whereas the bottom shows the corresponding solitary structure. Other parameters are $\Gamma = 0.4$, $\theta = 0.8\,\pi/2$, and $\beta = 0.1$.

for different values of Alfvén Mach number, and Figures 2 (bottom) and 3 (bottom) show the corresponding solitary structures. It is found that an increase in M_A leads to the reduction in the amplitude of the solitary kinetic Alfvén wave, and also decreases its width.

Figure 2 exhibits the variation of Sagdeev potential for decreasing values of κ in the electron distribution, and also plots the corresponding solitary structures (top and bottom, respectively). It can be seen that the amplitude and width of the solitary structures decrease with decreasing values of kappa parameter.

4.2. Existence Condition for Rarefactive Solitary Structures

We can also find negative potential or rarefactive solitons if the Sagdeev potential satisfies the following condition:

$$\sqrt{\frac{\beta}{2\gamma}} < M_A < k_z\sqrt{\frac{\eta}{\gamma^2+\eta}}. \tag{24}$$

Numerical solutions of equation (22) for the rarefactive solitary structures are plotted in Figures 4 and 5. Figure 4 manifests the variation of the Sagdeev potential for different values of Alfvén Mach number, and the bottom shows the corresponding solitary structures. It is found that an increase in M_A enhances the amplitude as well as width of the solitary kinetic Alfvén wave in terms of magnitude. Figure 5 investigates the variation of the Sagdeev potential for increasing values of κ, and also plots the corresponding solitary structures. It is observed that the increase in κ values leads to an increase in the amplitude as well as the width of the solitary structure.

It is worth mentioning here that equations (23) and (24) are general conditions for compressive and rarefactive solitons and hold true both for the kappa and *Cairns et al.* [1995] cases. However, the coefficients γ and η are defined differently for either case.

Numerical solutions of equation (22) are plotted in Figures 6 and 7 for the compressive solitary structures for *Cairns et al.* [1995] distributed electrons. Figure 6 explores the effect of M_A on the Sagdeev potential

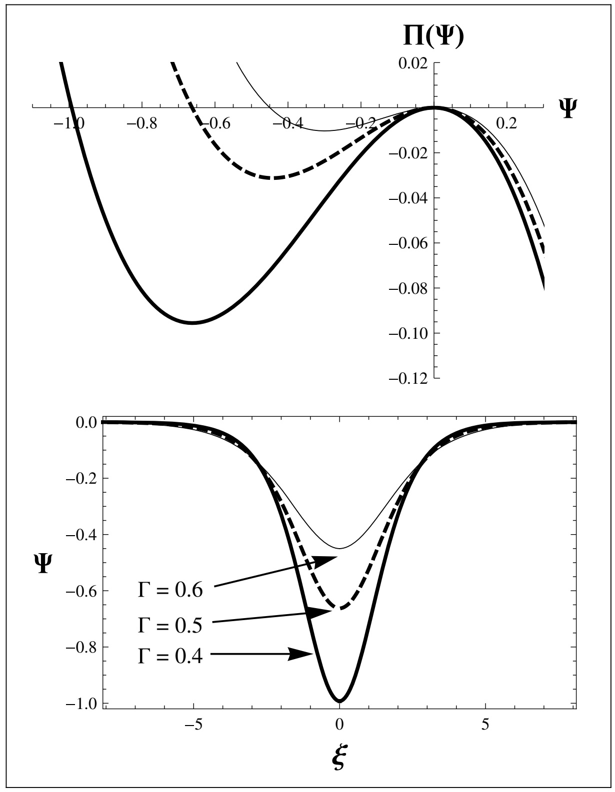

Figure 9. Variation of Sagdeev potential—*Cairns et al.* [1995] distributed electrons—for different values of $\Gamma = 0.4$ (solid line), $\Gamma = 0.5$ (dashed line), and $\Gamma = 0.6$ (thin line) are shown in the top, whereas the bottom shows the corresponding solitary structure. Other parameters are $M_A = 0.7$, $\theta = 0.8\,\pi/2$, and $\beta = 0.1$.

and the corresponding solitary structure. It is observed that the increasing M_A decreases the amplitude of the solitary structure while increasing its width, and the trend is similar to the one found in the case of kappa-distributed electrons. Figure 7 depicts the behavior of Sagdeev potential and the corresponding solitary structure as we vary the values of nonthermal parameter Γ for the *Cairns et al.* [1995] distributed electrons. It is found that an increase in the nonthermal electron population enhances the amplitude as well as the width of the solitary structure.

We plot the numerical solutions of equation (22) for the rarefactive solitary structures for *Cairns et al.* [1995] distributed electrons in Figures 8 and 9. Figure 8 investigates the effect of M_A on the Sagdeev potential and the corresponding solitary structure. It is found that increasing M_A enhances the amplitude as well as the width of the solitary structure of the kinetic Alfvén wave in terms of magnitude. Figure 9 exhibits the effect of increasing nonthermal parameter Γ on the rarefactive solitary structures for *Cairns et al.* [1995] distributed electrons. It is observed that an increase in nonthermal electron population in this case suppresses the amplitude of the solitary structure and brings about a decrease in width as well.

Finally, Figure 10 is plotted to show that the rarefactive solitons exist only for the kappa and *Cairns et al.* [1995] distributed electrons and they cease to exist for the Maxwellian electrons. Note that a certain threshold percentage of nonthermal electron population is required for the formation of rarefactive solitons. For instance, it can be seen that the rarefactive solitons appear for more than 20 % of nonthermal electrons in case of *Cairns et al.* [1995] distributed electrons. Similarly, for $\kappa = 2.2$, we see the formation of rarefactive electrons but for larger values of kappa, the rarefactive solitons cease to exist. It is worth mentioning here that the inclusion of the non-Maxwellian population alters the values of the Sagdeev potential (as given by equation (22)), leading to the new results obtained in this paper.

Moreover, since the parameter ξ is normalized by the ion-acoustic Larmor radius, it turns out that the scale length of the formation of solitary structures varies from one tenth of a kilometer to one twentieth of a kilometer. The SKAWs are one of the most attractive phenomena in the nonlinear plasma waves observed

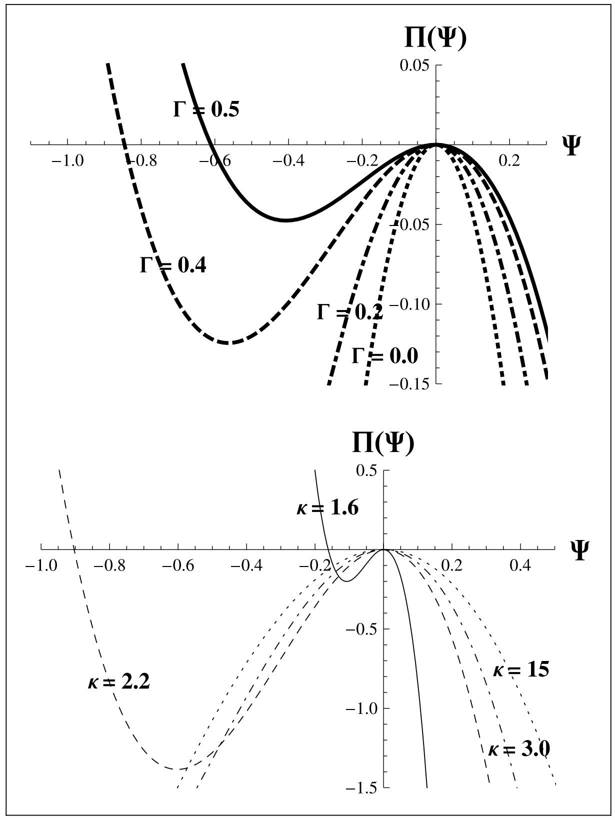

Figure 10. Rarefactive Sagdeev potential for both Cairns and Kappa-distributed electrons. It can be seen that as both distributions approach the Maxwellian limit ($T = 0$ and $\kappa \to \infty$), the rarefactive Sagdeev potential ceases to exist.

by the F4 experiment on the Freja satellite. The properties of these localized structures are introduced by *Louarn et al.* [1994]. The SKAWs are characterized as strong electromagnetic perturbations associated with a strong fluctuation of the plasma density. *Huang et al.* [1997] reported that some properties of SKAW's are still ambiguous. The major anomaly being the plasma density fluctuations which are not only compressive solitons but also rarefactive cavitons, which cannot be explained within the current framework of the SKAW's. Remarkably, the present two-fluid theory with non-Maxwellian electrons yields both the compressive and rarefactive solitary structures and explains the anomaly found in the plasma density fluctuations in the Freja satellite associated with the electromagnetic perturbations.

5. Summary and Conclusion

In this paper, we have studied the linear and nonlinear propagation of kinetic Alfvén waves in low-beta plasmas in the presence of kappa and *Cairns et al.* [1995] distributed electron population. Making use of the Sagdeev potential approach, we have studied the existence condition for the formation of the arbitrary amplitude solitary kinetic Alfvén wave and have found that solitons are formed for the sub Alfvénic mode, whereas no soliton is formed for the super Alfvénic mode. We have also explored the effects of the variation of nonthermal population for both kappa and *Cairns et al.* [1995] distributed electrons and Alfvén Mach number on the propagation characteristics of the nonlinear solitary structure of kinetic Alfvén waves.

In the present paper, we have utilized non-Maxwellian—kappa and *Cairns et al.* [1995]—models for the electrons to obtain both the compressive and rarefactive solitary kinetic Alfvén wave solutions for the first time. If one employs Maxwellian distribution for the electrons, then only compressive soliton solution can be obtained, as shown by previous works [*Hasegawa and Mima*, 1976; *Yu and Shukla*, 1978]. It is also shown that this study also solved the anomaly in the plasma density fluctuations associated with strong magnetic perturbations observed by the Freja satellite. The present investigation is an example which shows that the non-Maxwellian charged particle distributions in space plasma cannot only be used to better model the observation but also lead to a fundamentally new physical situation as compared to the plasma with thermal distributions. The present investigation may also be beneficial in understanding the propagation of solitary structures in diverse space environments where nonthermal populations of electrons have been observed and the low-beta plasma assumption holds true.

Acknowledgments
Numerical data for generating all the figures will be made available upon request (contact information: Waqas Masood [waqasmas@gmail.com]). M.N.S. Qureshi acknowledges the Higher Education Commission (HEC), Pakistan grant 20-1886/R&D10. P.H.Y. acknowledges NSF grants AGS1138720 and AGS1242331 to the University of Maryland, and the BK21-Plus grant to Kyung Hee University, Korea, from the National Research Foundation (NRF) funded by the Ministry of Education of Korea.

Michael Balikhin thanks the reviewers for their assistance in evaluating this paper.

References

Baluku, T. K., and M. A. Hellberg (2008), Dust acoustic solitons in plasmas with kappa-distributed electrons and/or ions, *Phys. Plasmas*, *15*, 123705, doi:10.1063/1.3042215.
Baluku, T. K., M. A. Hellberg, and R. L. Mace (2011), Electron acoustic waves in double-kappa plasmas: Application to Saturn's magnetosphere, *J. Geophys. Res.*, *116*, A04227, doi:10.1029/2010JA016112.
Bostrom, R. (1992), Observations of weak double layers on auroral field lines, *IEEE Trans. Plasma Sci.*, *20*, 756–763, doi:10.1109/27.199524.
Cairns, R. A., A. A. Mamun, R. Bingham, R. Boström, R. O. Dendy, C. M. C. Nairn, and P. K. Shukla (1995), Electrostatic solitary structures in non-thermal plasmas, *Geophys. Res. Lett.*, *22*, 2709–2712.
Carlson, C. W., J. P. McFadden, and R. E. Ergun (1998), FAST observations of ionospheric processes responsible for the aurora, American Physical Society, Division of Plasma Physics Meeting, New Orleans, La., 16-20 Nov.
Christon, S. P., D. G. Mitchell, D. J. Williams, L. A. Frank, C. Y. Huang, and T. E. Eastman (1988), Energy spectra of plasma sheet ions and electrons from about 50 eV/e to about 1 MeV during plasma temperature transitions, *J. Geophys. Res.*, *93*, 2562–2572, doi:10.1029/JA093iA04p02562.
Delamere, P. A., and F. Bagenal (2008), Longitudinal plasma density variations at Saturn caused by hot electrons, *Geophys. Res. Lett.*, *35*, L03107, doi:10.1029/2007GL031095.
Dovner, P. O., A. I. Eriksson, R. Bostrom, and B. Holback (1994), Freja multiprobe observations of electrostatic solitary structures, *Geophys. Res. Lett.*, *21*, 1827–1830.
Hall, J. O., P. K. Shukla, and B. Eliasson (2005), Structure formation by modulational interactions between lower-hybrid and dispersive Alfvén waves, *Phys. Plasmas.*, *12*, 52,310, doi:10.1063/1.1896373.
Hasegawa, A., and K. Mima (1976), Exact solitary Alfvén wave, *Phys. Rev. Lett.*, *37*, 690, doi:10.1103/PhysRevLett.37.690.
Hasegawa, A., and C. Uberoi (1982), *The Alfven Wave*, DOE Critical Review Series-Advances in Fusion Science and Engineering Technical Information Center, U.S. Department of Energy, Washington, D. C.
Hasegawa, A., K. Mima, and M. Duong-van (1985), Plasma distribution function in a superthermal radiation field, *Phys. Rev. Lett.*, *54*, 2608, doi:10.1103/PhysRevLett.54.2608.
Hellberg, M. A., R. L. Mace, T. K. Baluku, I. Kourakis, and N. S. Saini (2009), Comment on "Mathematical and physical aspects of Kappa velocity distribution", *Phys. Plasmas*, *16*, 094701, doi:10.1063/1.3213388.
Huang, G.-L., D.-Y. Wang, D.-J. Wu, H. de Féraudy, D. Le Quéau, M. Volwerk, and B. Holback (1997), The eigenmode of solitary kinetic Alfvén waves observed by Freja satellite, *J. Geophys. Res.*, *102*, 7217, doi:10.1029/96JA02607.
Kadomtsev, B. B. (1965), Plasma turbulence, *New York*, 82 pp.
Krimigis, S. M., J. F. Carbary, E. P. Keath, T. P. Armstrong, L. J. Lanzerotti, and G. Gloeckler (1983), General characteristics of hot plasma and energetic particles in the Saturnian magnetosphere—Results from the Voyager spacecraft, *J. Geophys. Res.*, *88*, 8871–8892.
Livadiotis, G., and D. J. McComas (2013), Understanding kappa distributions: A toolbox for space science and astrophysics, *Space Sci. Rev.*, *175*, 183–214.
Louarn, P., et al. (1994), Observation of kinetic Alfvén waves by the FREJA spacecraft, *Geophys. Res. Lett.*, *21*(17), 1847–1850, doi:10.1029/94GL00882.
Ma, C.-Y., and D. Summers (1998), Formation of power-law energy spectra in space plasmas by stochastic acceleration due to whistler-mode waves, *Geophys. Res. Lett.*, *25*, 4099.
Maksimovic, M., V. Pierrard, and J. F. Lemaire (1997), A kinetic model of the solar wind with kappa distribution functions in the corona, *Astron. Astrophys.*, *324*, 725–734.
Pierrard, V., and M. Lazar (2010), Kappa distributions: Theory and applications in space plasmas, *Sol. Phys.*, *267*, 153–174.
Pierrard, V., and J. Lemaire (1996), Lorentzian ion exosphere model, *J. Geophys. Res.*, *101*, 7923–7934.
Pierrard, V., H. Lamy, and J. F. Lemaire (2004), Exospheric distributions of minor ions in the solar wind, *J. Geophys. Res.*, *109*, A02118, doi:10.1029/2003JA010069.
Scudder, J. D., and S. Olbert (1979), A theory of local and global processes which affect solar wind electrons. II—Experimental support, *J. Geophys. Res.*, *84*, 6603–6620, doi:10.1029/JA084iA11p06603.
Schippers, P., et al. (2008), Multi-instrument analysis of electron populations in Saturn's magnetosphere, *J. Geophys. Res.*, *113*, A07208, doi:10.1029/2008JA013098.
Stasiewicz, K., et al. (2000), Small scale Alfvénic structure in the aurora, *Space Sci. Rev.*, *92*, 423.
Summers, D., and R. M. Thorne (1991), The modified plasma dispersion function, *Phys. Fluids B*, *3*, 1835, doi:10.1063/1.859653.
Vasyliunas, V. M. (1968), A survey of low-energy electrons in the evening sector of the magnetosphere with OGO 1 and OGO 3, *J. Geophys. Res.*, *73*, 2839–2884.
Viñas, A. F., R. L. Mace, and R. F. Benson (2005), Dispersion characteristics for plasma resonances of Maxwellian and Kappa distribution plasmas and their comparisons to the IMAGE/RPI observations, *J. Geophys. Res.*, *110*, A06202, doi:10.1029/2004JA010967.
Voitenko, Y., and M. Goossens (2005), Cross-scale nonlinear coupling and plasma energization by Alfvén waves, *Phys. Rev. Lett.*, *94*, 135,003, doi:10.1103/PhysRevLett.94.135003.
Voitenko, Y., M. Goossens, O. Sirenko, and A. C.-L. Chian (2003), Nonlinear excitation of kinetic Alfvén waves and whistler waves by electron beam-driven Langmuir waves in the solar corona, *Astron. Astrophys.*, *409*, 331–345.
Yinhua, C., L. Wei, and M. Y. Yu (2000), Nonlinear dust kinetic Alfvén waves, *Phys. Rev. E.*, *61*, 809, doi:10.1103/PhysRevE.61.809.
Yoon, P. H. (2012), Electron kappa distribution and steady-state Langmuir turbulence, *Phys. Plasmas*, *19*, 52,301, doi:10.1063/1.4710515.
Yoon, P. H. (2014), Electron kappa distribution and quasi-thermal noise, *J. Geophys. Res*, *119*, 7074–7087, doi:10.1002/2014JA020353.
Yoon, P. H., L. F. Ziebell, R. Gaelzer, and R. P. Lin (2012), Langmuir turbulence and suprathermal electrons, *Space Sci. Rev.*, *173*, 459–489.
Yu, M. Y., and P. K. Shukla (1978), Finite amplitude solitary Alfvén waves, *Phys. Fluids*, *21*, 1457, doi:10.1063/1.862368.
Yu, M. Y., P. K. Shukla, and A. C. Das (1984), Decay of electrostatic ion cyclotron waves, *Geophys. Res. Lett.*, *11*, 16–18.
Zhao, J. S., D. J. Wu, and J. Y. Lu (2011), Kinetic Alfvén waves excited by oblique magnetohydrodynamic Alfvén waves in coronal holes, *Astrophys. J.*, *735*, 114, doi:10.1088/0004-637X/735/2/114.

